View metadata, citation and similar papers at core.ac.uk
brought to you by CORE
provided by UNT Digital Library

Ion Implanted Ge:B Far Infrared Blocked Impurity Band Detectors

Jeffrey W. Beeman[b], Supriya Goyal[a,b], Lothar A. Reichertz[a,b], Eugene E. Haller[*a,b]
[a]University of California, Berkeley and [b]Lawrence Berkeley National Laboratory,
Berkeley, CA 94720

Ge Blocked Impurity Band (BIB) photoconductors have the potential to replace stressed Ge:Ga photoconductors for far-infrared astronomical observations. A novel planar BIB device has been fabricated in which ion-implanted boron is used to form the blocking and absorbing layers of necessary purity and compensation. The effect of doping in the infrared active layer on the far-infrared photoconductive response has been studied, and the optimum doping concentration is found to be ~ $4x10^{16}$ cm^{-3}. Devices doped near this concentration show good blocking characteristics with low dark currents. The spectral response extends to ~ 45 cm^{-1}, clearly showing the formation of an impurity band. Under low background testing conditions these devices attain a responsivity of 0.12 A/W and NEP of 5.23 x 10^{-15} $W/Hz^{-1/2}$.

Keywords: germanium, blocked impurity band detector, far infrared, photoconductor, ion implantation

PACS-2006 codes: 85.60.Gz, 07.57.Kp

1. INTRODUCTION

For astronomers and astrophysicists, the far-infrared (FIR) region of the electromagnetic spectrum (spectral range 40-1000 μm) holds a great wealth of information for understanding many aspects of the universe[1,2,3]. The peak of the blackbody emission from many low temperature objects in space such as planets, infrared galaxies, newly forming stars, nebulae and brown dwarfs lies in the mid to far-infrared. However, in this wavelength range atmospheric transmission is extremely low, primarily due to excitation of vibrational and rotational modes of various molecules in the atmosphere such as H_2O, O_2, O_3, CO_2, N_2O, and CH_4[4]. In addition, a far-infrared detector on a ground-based ambient temperature telescope receives a strong background flux of

* Corresponding author. E-mail: EEHaller@lbl.gov

thermal emission from the telescope and the atmosphere[5]. This poses a serious problem for FIR astronomy and exploration of FIR must be performed from high altitudes where the atmosphere is of low density or from outer space.

Primary technologies for detection in the FIR use extrinsic semiconductor photoconductors and bolometers[6]. Photoconductors have been developed that can detect energies down to 6 meV (~200 μm, 50 cm^{-1}), corresponding to the ionization energies of shallow donors (for example, donors in GaAs) and acceptors (for example, acceptors in stressed Ge) in semiconductors. At lower energies (< 6 meV) where there are no suitable photoconductors, bolometers (thermal sensors) must be used. Bolometers will not be discussed here in detail as they are fundamentally different in operation from photoconductors and pose serious challenges for integration onto arrays for space based telescopes.

Extrinsic photoconductors are doped semiconductors that detect light as a measured change in photocurrent when electrons (holes) are excited from the dopant ground state into the conduction (valence) band. The minimum detectable energy corresponds to the binding energy of the electron (hole) to the donor (acceptor). Shallow dopant binding energies in Ge are of the order of 10 meV, suitable for FIR detectors. Ga acceptors in Ge have an ionization energy of about 11 meV, corresponding to a cutoff wavelength of about 113 μm[7]. The response of Ge:Ga photoconductors can be extended to longer wavelengths (~ 200 μm, 50 cm^{-1}) by applying a uniaxial compressive stress[8], which has the effect of splitting the four-fold degeneracy of the Γ_4 valence band edge and reducing the energy difference between the bound acceptor states and the top of the valence band[9]. The drawback of stressed Ge detectors is the difficulty in fabricating a stress mechanism for large two-dimensional arrays.

Ge Blocked Impurity Band (BIB) detectors have the potential to detect energies as low as 6 meV without the need for applying stress. The BIB detector has been implemented in Si, lowering the detection onset to ~ 30 meV (~ 41 μm)[10]. A 128x128 pixel Si BIB array is part of the Multiband Imaging Photometer currently onboard the Spitzer Space Telescope (MIPS)[11] that is used to detect radiation near 417 cm^{-1} (24 μm). The Si BIB devices and their corresponding readout electronics operate at a relatively easily obtainable temperature of 6 K.

A schematic of a p-type Ge BIB is shown in Figure 1. The FIR absorbing layer of the device is heavily doped Ge, where considerable orbital overlap between the individual impurity levels has caused them to merge into an impurity band. Impurity band broadening reduces the acceptor excitation energy and allows response to lower energy photons. If this heavily doped FIR layer were used as such in a photoconductor, the device would incur a high dark current because holes would move in the impurity band even though they would not have enough energy to enter the valence band. This dark current would cause noise far above the signal level. To overcome this problem, the BIB detector uses a high purity blocking layer inserted between the absorbing layer and one of the electrical contacts.

The operation of the BIB device can be understood from Figure 1. Although in this example the absorbing layer is a p-type semiconductor, it will always contain compensating n-type impurities. These donors lose electrons to the acceptors, leaving ionized donor and acceptor states distributed throughout the layer. When an electric field is applied, the holes move in the impurity band towards the negative contact, where they are stopped by the blocking layer (because no impurity band exists in the blocking layer). The holes thereby fill the ionized acceptor states closest to the FIR layer- blocking layer interface. In this region there will be a net space charge due to the positively charged impurity donors. The resulting depletion width (w) is the active region of the device where absorbed light excites holes from the impurity band into the valence band where they move through the blocking layer and are collected at the negative contact. At the same time, the ionized acceptor state A^- created in this ionization event moves towards and is collected at the positive electrode. The collection of both the hole and the ionized acceptor state results in unity photoconductive gain.

The Ge BIB detector will have several advantages compared to bulk photoconductors. The high doping concentration affords the advantage of lowering the minimum detectable photon energy due to impurity band broadening. In addition, the optical absorption coefficient (α) of the FIR absorbing layer is also higher due to the increased doping concentration, therefore a thinner layer than used in standard photoconductors is sufficient for efficient photon absorption. The resulting reduction in total detector volume of about 100 times compared to standard photoconductors decreases the rate of cosmic radiation “hits” during device operation. As mentioned

before, unity photoconductive gain can be achieved in the BIB detector. Unity gain, in contrast to gain distribution found in standard photoconductors, leads to lower generation-recombination noise.

For efficient functioning of the BIB detector, there are stringent demands placed on the dopant concentrations and layer thicknesses. The FIR absorbing layer must have a dopant with low ionization energy for long wavelength detection. The active layer of the BIB should be doped to a level where impurity band conduction occurs. For shallow dopants in Ge, banding begins at $\sim 10^{16}$ cm^{-3} and metallic conductivity occurs at $\sim 10^{17}$ cm^{-3}. Both the optical absorption and the photoconductive response of the BIB are expected to increase as the doping concentration increases. Ideally, it would be possible to tailor the onset of spectral response to any value between zero and the ionization energy. There are expected to be some practical limitations, for example local fluctuations in concentration could leave some regions metallic even if the overall concentration is not. For a given operating temperature, the dark current will become unacceptably large for very low energies between the dopant band and the valence band edge. However, it should be reasonable to achieve a photoconductive onset of ~ 6 meV (as low as stressed Ge:Ga detectors).

In addition to the (majority) acceptor concentration, the (minority) donor concentration has an important effect on the proper functioning of a BIB device. Only carriers generated within the depletion layer are driven by the applied electric field into the blocking layer, so it is beneficial to have thick depletion layer. The width of the depletion layer depends on the minority dopant concentration (N_{min}) and the applied voltage (V_{a}), which is derived from the Poisson equation. Petroff and Staplebroek included the blocking layer thickness in their derivation of the equation for depletion layer width[12]:

$$w = \left[\sqrt{\frac{2\varepsilon\varepsilon_0 V_a}{eN_{\mathrm{min}}} + b^2} \right] - b \qquad (1)$$

where e = electron charge, ε_{o} = permittivity of free space, ε = dielectric constant of Ge, b = blocking layer thickness. For a fixed applied voltage, a low N_{a} and small b are desirable to keep the depletion width large.

The blocking layer of a Ge BIB device must be thin (1-10 μm), and high purity ($N_{\mathrm{a}} < 10^{13}$ cm^{-3}). High performance Ge:Ga photoconductors typically contain Ga concentrations of between $1\mathrm{x}10^{14}$ and $3\mathrm{x}10^{14}$ cm^{-3}.

These concentrations are below the onset of significant hopping conduction. Such devices maintain dark currents of a few hundred electrons per second or less under standard operating conditions. It would therefore seem appropriate that the blocking layer of a BIB device should be of similar concentration. However, numerical modeling by Haegel, et. al.[13] has shown that the electric field distribution in the BIB creates a more stringent requirement of $< 10^{13}$ cm^{-3} for the blocking layer.

Motivated by the success of Si BIB detectors (discussed in section 1.4), there have been several attempts to implement these devices in Ge. Initial efforts to grow Ge BIB structures focused on chemical vapor deposition (CVD) of Ge:Ga[14,15]. The devices fabricated showed response down to 50 cm^{-1} (200 μm), however results were not reproducible and the detectors suffered from large dark currents due to unpassivated surfaces. Preliminary results from devices fabricated with Liquid Phase Epitaxy (LPE) grown Ge films using Pb as a solvent were encouraging showing some extended wavelength response [16]. The purity of commercially available Pb was found to be a problem, with n-type impurities ~ 10^{15} cm^{-3}, identified by photothermal ionization spectroscopy to be phosphorus. Such dopant concentrations were too high for growth of the pure blocking layer, therefore a BIB device was made by growth of a doped active layer on a pure substrate, and polishing back the substrate to form the blocking layer[17]. These devices exhibited significant Sb diffusion into the pure substrate during growth. BIB modeling[13] indicates that the Sb gradient at the absorbing layer – blocking layer interface would increase the electric field in the transition region and reduce the field in the blocking layer. This spike in the electric field at the active layer – blocking layer interface is believed to enhance device breakdown at lower applied biases. In addition, the depletion width of the BIB device is expected to have a lower Sb concentration than the absorbing layer, leading to a reduction in the long wavelength response. Ge BIB detectors based on films grown by LPE show good blocking characteristics at low temperatures, but the optical response is severely limited by the inability to grow a blocking layer of required purity and the lack of an abrupt interface between the active and blocking layers due to Sb diffusion at the interface during growth.

To achieve the goals of high purity (for the blocking layer), low compensation (for the absorbing layer) and an abrupt interface between the absorbing and blocking regions, a new kind of BIB device has been designed and fabricated. The necessary doped layers are created via ion-implantation. Starting with ultra-pure, optically

polished crystalline Ge, lithographic masking, ion implantation, and metallization have been used to produce the infrared absorbing, blocking and contact regions. The resulting device is referred to as an Ion-implantation Blocked Impurity Band detector (IBIB).

2. EXPERIMENTAL PROCEDURES

The processing steps in the fabrication of an IBIB device are shown schematically in Figure 2. The IBIB is a planar device fabricated using only near surface processing techniques. As mentioned before, the starting material is a high purity (~$1x10^{11}$ cm^{-3}) Ge substrate, which also serves as the blocking region of the device. The Ge wafer wafer was polished with 7:3:1 H_2O:syton (colloidal silica):H_2O_2 on a polishing pad. Positive photoresist (S1818) from Shipley[1] was spun on the Ge wafer at 4000 RPM for 30 s. The photoresist was soft baked at 90°C for 30 s, followed by a pre-soak in developer (Shipley LDD26W) for 60 s. This was followed by a rinse with distilled H_2O and blow-drying with N_2 gas. The mask in Figure 2 was aligned onto the Ge substrate using a Q2001 Mask Aligner from Quintel Corporation[2] and the the photoresist was exposed to UV light at 100 mJ/cm^2 for 28 s. The photoresist was then developed in Shipley LDD26W; the sample was rinsed with distilled H_2O and blow-dried. 200 Å of Pd and 4000 Å of Au were deposited using electron-beam evaporation to form the alignment marks (that serve as a reference for future patterning steps). The photoresist was stripped by sonicating the sample in acetone for 30 minutes. The patterns for the infrared active region and contact region were created using the same processing steps. Ion implanted boron was used to form the absorbing and contact regions of the device. Using this technique, several sets of IBIB devices with absorbing region concentrations ranging from $1x10^{16}$ cm^{-3} to $5x10^{16}$ cm^{-3} have been prepared. The electrical contacts in each case were identical: a series of implants similar to the ones shown in Figure 2, but with higher doses to create metallic regions in the Ge. During the final mask procedure, Pd and Au were evaporated onto the contact regions to provide points of contact for wedge bonded wires. Figure 3 shows a fully processed wafer and single unit cell photoconductor.

Several important factors need to be considered in choosing an implant species for IBIB fabrication. The requirements for an efficient BIB detector necessitate the use of a shallow dopant species for long wavelength

---

[1] Shipley Company, LLC. 455 Forest Street, Marlborough, MA 01752.
[2] Quintel Corporation. 2431 Zanker Road, San Jose, CA 95131.

detection; since the material used for the blocking region is p-type Ge, the implant species must also be a p-type dopant in Ge. In addition, the implanted species should travel far into the crystal surface creating a thick active region for efficient absorption of light. Boron (ionization energy 10.82 meV) with an atomic mass of 10 or 11 amu travels the furthest (per keV of accelerator voltage) of all the shallow dopants in Ge, and was therefore chosen as the implanted dopant species. An added advantage of using B is that being light, it causes relatively little crystalline damage. The small amount of crystalline damage caused by the light B mass can be annealed by using relatively low temperatures (450°C) during processing. This is particularly important for Ge since a higher temperature annealing can sometimes produce interstitial Cu donor species[18] that would compensate the B, leading to poor depletion and device performance. If any damage remains after annealing, it will not compensate the B acceptors as this damage tends to be p-type in Ge.

3. RESULTS AND DISCUSSION

Figure 4 shows a representative series of implants and the resulting B concentration as a function of depth for the infrared absorbing region of an IBIB device with a peak B concentration of $4x10^{16}$ cm^{-3} in the active layer. The presence of B has been confirmed by SIMS; Figure 5 shows a comparison of the B concentration expected from implant simulation and the measured concentration obtained by SIMS analysis. In addition, Hall effect measurements on Ge wafers implanted with B ions (similar doses and implant energies) and annealed at 450°C show that the B implanted in the infrared absorbing region is electrically active.

The dark current-voltage characteristics of the Ge BIB device for several temperatures are shown in Figure 6. The I-V curves for the BIB device are shown with negative bias applied to the blocking region. The device exhibits good blocking characteristics, and the leakage current is generally below 10^{-14} A, the detection limit of our electronics. A plateau is seen in the I-V curve due to the presence of the blocking layer which prevents conduction in the impurity band. It is well known that in a semiconductor at low temperatures, free carriers are “frozen-out” or bound to their respective impurity atoms. At 4 K, a few holes within the absorbing layer are not yet bound to acceptor impurities. These holes, which occupy the valence band, are free to travel through the blocking layer and constitute a dark current. Therefore, the dark current is only slightly reduced by the

presence of the blocking layer at 4 K. As the temperature is reduced, however, more holes become bound within the impurity band of the absorbing layer, and are therefore blocked from traveling through the blocking layer where no impurity band exists. At 2.2 K, the dark current through the BIB device is greatly reduced, finally at at 1.2 K, the I-V curve is nearly constant over a wide bias range, indicating the efficient blocking of holes from the absorbing layer.

Far infrared spectra of the Ge IBIB devices were recorded using a Fourier transform infrared spectrometer. The spectra were recorded using a 0.001" Mylar beamsplitter and an 8 mil black polyethylene filter to eliminate band gap light. The dip in the intensity at ~ 170 cm^{-1} is due to a beamsplitter resonant absorption. The photoconductivity spectra of two Ge IBIB devices (with peak doping concentrations of $1x10^{16}$ cm^{-3} and $4x10^{16}$ cm^{-3} in the absorbing layer) measured at 1.3 K with a -30 mV negative bias applied to the blocking layer are shown in Figure 7. It is seen that with higher doping the response extends to longer wavelengths due to the broadening of the impurity band. The response in both cases extends to longer wavelengths than Ge:Ga photoconductors. The sharp line seen at 64.5 cm^{-1} in the spectrum for IBIB 3 is the 'D' line for B in Ge, which is assigned to the 1s-2p transition[19,20]. The signal to noise ratios were > 1000 and the absolute signal sizes were tens of millivolts, which was somewhat unexpected since our current mask design results in only ~ 40% active area. In addition, for a device with $4x10^{16}$ cm^{-3} doping (α = 300 cm^{-1}) and an active region of 1μm thickness (the thickness of the implant), the absorption efficiency is only 1.2%. However, these effects are offset in our test detectors by a relatively large incident absorbing surface of 6.4 mm^2. Since the IBIB device with a peak concentration of $4x10^{16}$ cm^{-3} showed the largest extension in long wavelength response, additional measurements were performed on this device using a low-pass filter[21] with a cutoff at 107 cm^{-1} and a transmission of 90%. The spectral response of the device under these testing conditions is shown in Figure 8. The spectra were of good enough quality to observe distinctly the extension in long wavelength photoconductive response to ~ 45 cm^{-1}. Devices with peak doping ~ $6x10^{16}$ cm^{-3} in the active region exhibit high dark currents, indicating the impurity band has merged with the valence band at this high doping concentration.

The $4x10^{16}$ cm^{-3} device was also tested under low background conditions to measure performance under more typical astronomical observation conditions. With the detector cooled to 1.3 K and using a chopped, 3.4 x 10^{-12} W signal that was narrow band filtered at 90 microns wavelength, this device achieved a responsivity of 0.12 A/W and NEP of 5.23 x 10^{-15} $W/Hz^{-1/2}$. While this is below the performance of current state-of-the-art photoconductors, we feel this result is still respectable given the shallow nature of the ion implant.

4. CONCLUSION

We have fabricated a new type of device, an ion-implantation Blocked Impurity Band detector (IBIB), in which lithographic masking, boron ion-implantation, and metallization have been used to produce the infrared absorbing, blocking and contact regions. These devices exhibit low dark currents and excellent blocking characteristics. The photoconductive response for all devices tested extends to longer wavelengths than standard Ge:Ga photoconductors; for devices with a doping concentration of $4x10^{16}$ cm^{-3} in the infrared active layer the response extends to ~45 cm^{-1}. The responsivity and NEP of these devices does not match that of Ge:Ga photoconductors, which is not surprising given the shallow nature of the ion implant and the consequently thin absorbing region. We are confident that with schemes to improve the absorption efficiency (e.g. by increasing the width of the absorption region, using higher energy implants or stacking devices) Ge IBIB detectors will reach competitive performance.

ACKNOWLEDGMENTS

This work was supported by the National Aeronautics and Space Administration, Interagency Agreement No. W-19,889 through the U.S. Department of Energy under Contract No. DE-AC03-76SF00098. SG acknowledges the financial support of the UC Berkeley Graduate Opportunity Fellowship and the Intel Foundation Ph.D. Fellowship.

REFERENCES

[1] D. Lemke, M. Stickel, K. Wilke (Eds.), *ISO Surveys of a Dusty Universe* (Springer-Verlag, Germany, 2000).

[2] G. Pilbratt, Infrared Phys. Technol., **35**, (2/3), 407 (1994).

[3] C. H. Townes, R. Genzel, Scientific American, **262** (4), 46 (1990).

[4] W. A. Traub and M. T. Stier, Applied Optics, **15**, 364 (1976).

[5] G. H. Rieke, M.W. Werner, R.I. Thompson, E.E. Becklin, W.F. Hoffman, J.R. Houck, W.A. Stein, F.C. Witteborn, Science, **231**, 807 (1986).

[6] E.E. Haller, Infrared Phys. Technol., **35** (2/3), 127 (1994).

[7] E.E. Haller, W.L. Hansen, F.S. Goulding, IEEE Trans. Nucl. Sci., **NS-22**, 127 (1975).

[8] A. G. Kazanskii, P. L. Richards, and E. E. Haller. Far-infrared photoconductivity of uniaxially stressed germanium. Appl. Phys. Lett., **31**, 496 (1977).

[9] H. Hasegawa, Physical Review, **129**, 1029 (1963).

[10] J.E. Huffman, A.G. Crouse, B.L. Halleck, T.V. Downes, J. Appl. Phys., **72** (1), 273 (1992).

[11] G. B. Heim, M. L. Henderson, K. I. Macfeely, T. J. Mcmahon, D. Michika, R. J. Pearson, G. H. Rieke, J. P. Schwenker, D.W. Strecker, C.L. Thompson, R.M. Warden, D. A. Wilson, E. T. Young. Multiband imaging photometer for SIRTF. *Proceedings of the SPIE*, **3356**:985-1000, (1998).

[12] M.D. Petroff, M.G. Stapelbroek, IRIS Specialty Group on IR Detectors, Seattle, WA (1984).

[13] N.M. Haegel, J.E. Jacobs, A.M. White. Applied Physics Letters, **77**, 4389 (2000).

[14] D.M. Watson, M.T. Guptill, J.E. Huffman, T.N. Krabach, S.N. Raines, S. Satyapal, J. Appl. Phys., **74**(6), 4199 (1993).

[15] J.E. Huffman, N.L. Casey, J. Crystal Growth, **129**, 525 (1993).

[16] C.S. Olsen, J.W. Beeman, W.L. Hansen, E.E. Haller, in *Infrared Applications of Semiconductors II. Symposium, Boston, MA, 1-4 Dec. 1997*, edited by D.L. McDaniel, Jr.et al., Mat. Res. Soc. Proc., **484**, 215 (1998).

[17] J. Bandaru, J.W. Beeman, E.E. Haller, S. Samperi, N.M. Haegel, Infrared Phys. Technol., **43**, 353 (2002).

[18] G. Sirmain, O.D. Dubon, W.L. Hansen, C.S. Olsen, E.E. Haller. A copper-related acceptor complex in vacuum grown germanium crystals. *Journal of Applied Physics*, **29**: 209-213, (1996).

[19] R.L. Jones, P. Fisher. Excitation spectra of group III impurities in germanium. *Journal of Physics and Chemistry of Solids*, **26**: 1125-1131, (1965).

[20] E.E. Haller, W.L. Hansen, Solid State Communications, **15**, 687 (1974).

[21] ‘C89’ long pass filter received from P. Ade, School of Physics and Astronomy, Cardiff University, Cardiff, Wales, U.K.

FIGURE CAPTIONS

Figure 1: Schematic of a p-type Blocked Impurity Band detector with band diagram below, shown for an electric field applied. Heavily doped contacts are labeled p^{++}. A^- = ionized acceptor, A^0 = neutral acceptor, D^+ = ionized donor, *w* = depletion width, *b* = blocking layer thickness.

Figure 2: The design and fabrication of an ion-implantation based BIB (IBIB) device. The blocking regions and IR active regions are 25 μm and 75 μm wide respectively.

Figure 3: Ge wafer with complete IBIB processing and a single "unit cell" from this wafer.

Figure 4: A representative series of implants for the infrared absorbing region of an IBIB device (IBIB 5). The solid line is the sum of all the implants and indicates the peak concentration (4×10^{16} cm^{-3}) of B in the active region of the device.

Figure 5: Calculated and measured B concentration vs. depth into Ge crystal surface for the infrared absorbing region of an IBIB device (IBIB 7).

Figure 6: Dark current-voltage characteristics of a Ge IBIB (IBIB 5) as a function of temperature.

Figure 7: Photoconductive response vs. wavelength for two IBIB devices (IBIB 3 and 5), with peak doping concentrations of 1×10^{16} cm^{-3} and 4×10^{16} cm^{-3} in the IR active layer respectively.

Figure 8: Spectral response for IBIB 5 with a long pass filter.

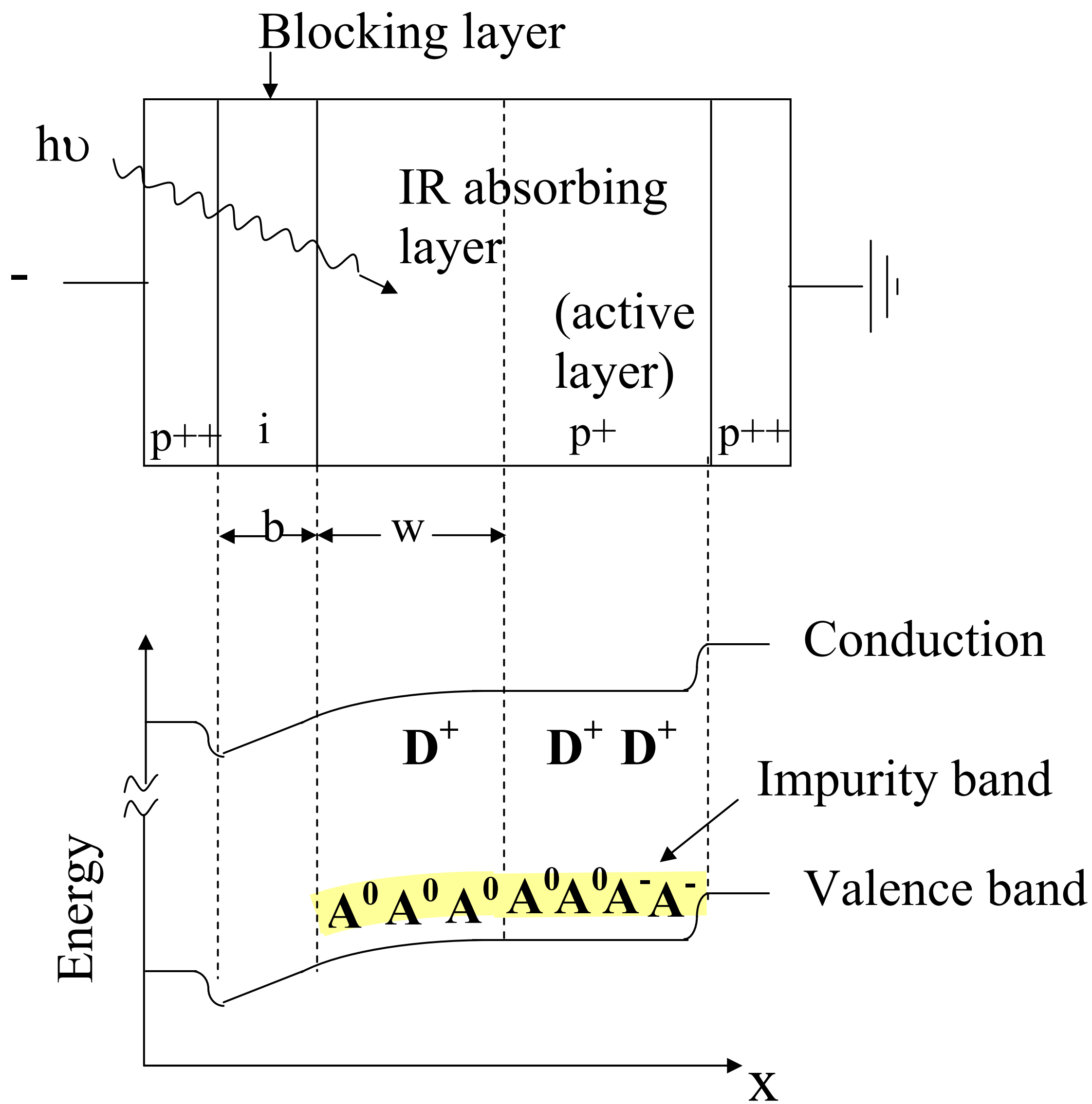

Figure 1
J. Beeman et al.

Step 1: Mask, deposit gold "alignment marks", strip photoresist

Step 2: Mask, Implant "IR active region" (~ 4×10^{16} cm^{-3} B), strip photoresist and anneal at 450°C to activate B and remove implantation damage

Step 3: Mask, ion-implant contact region and evaporate gold contacts. Strip photoresist when finished

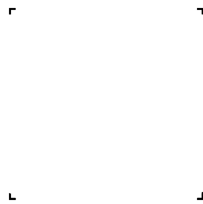

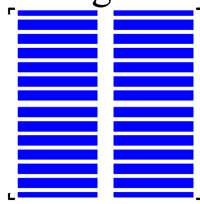

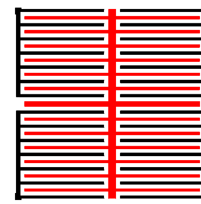

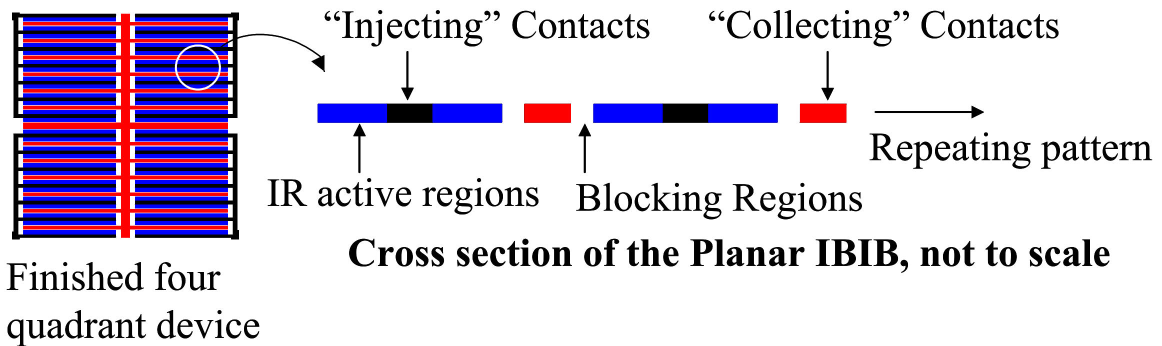

Cross section of the Planar IBIB, not to scale

Figure 2
J. Beeman et al.

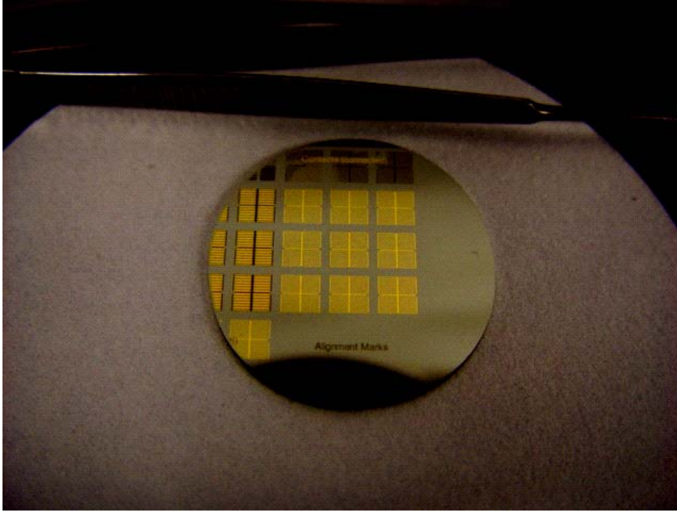

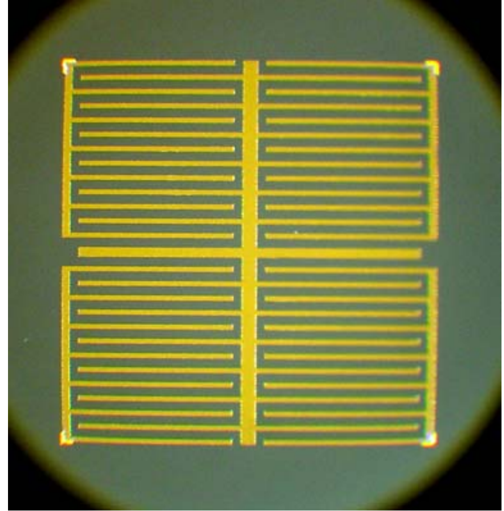

Figure 3
J. Beeman et al.

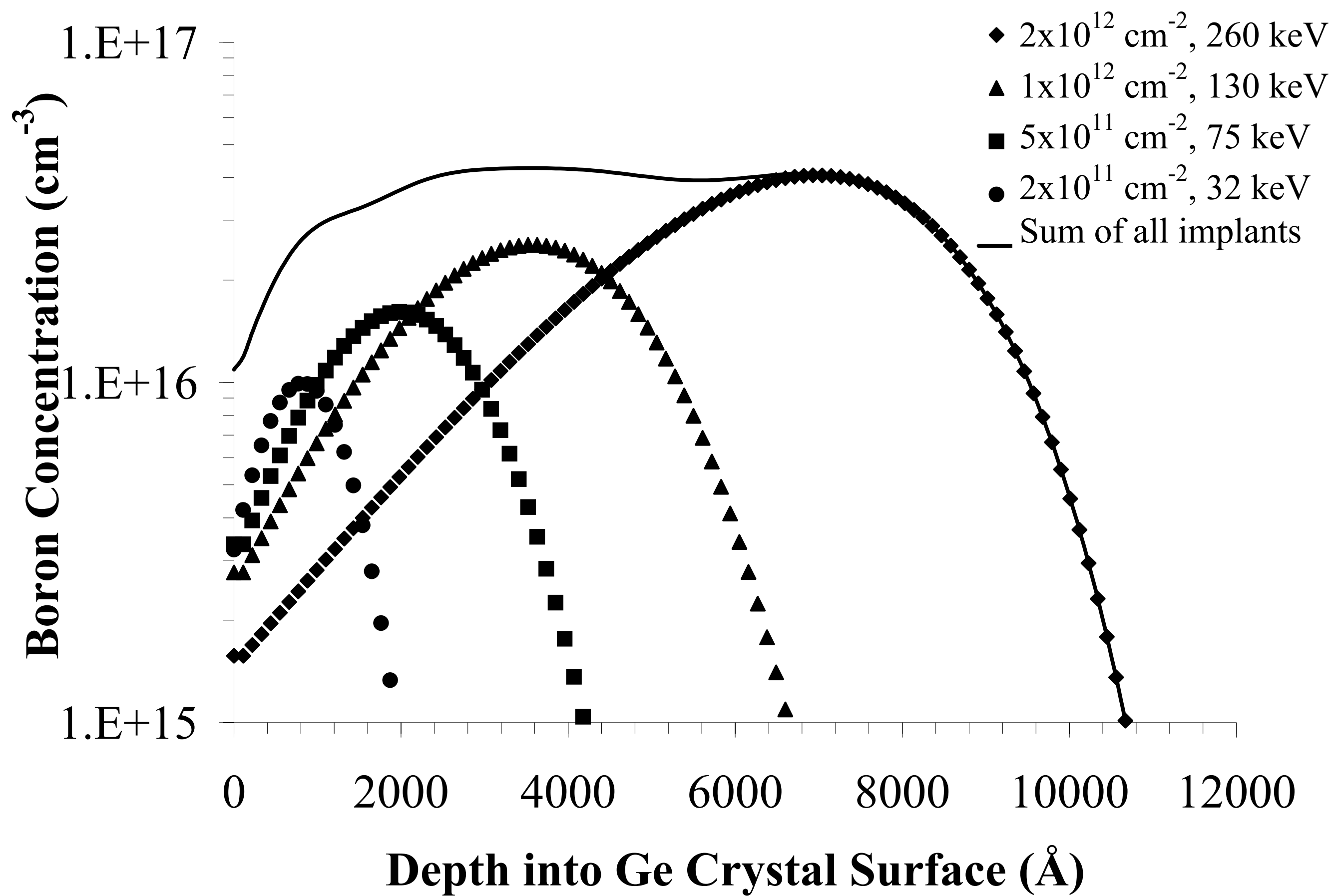

Figure 4
J. Beeman et al.

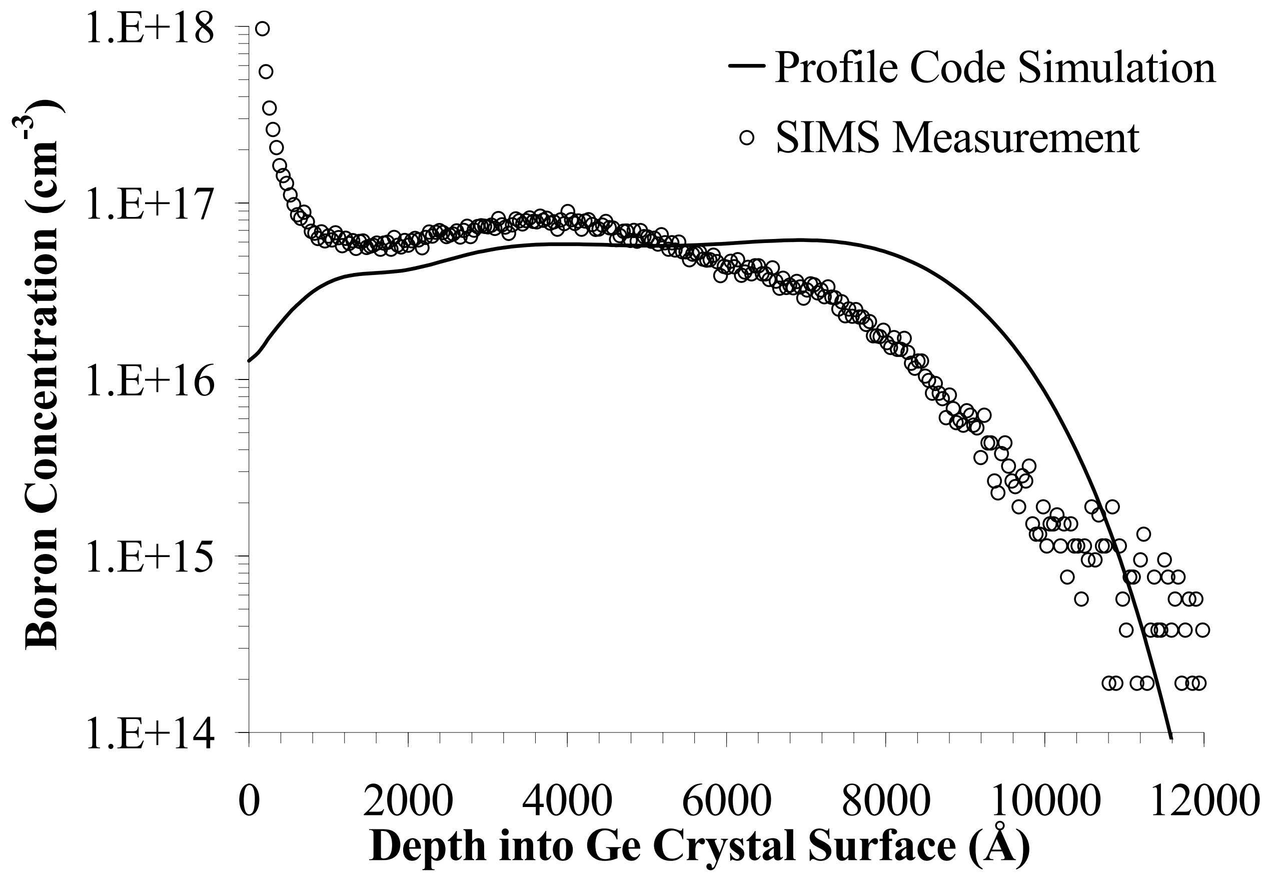

Figure 5
J. Beeman et al.

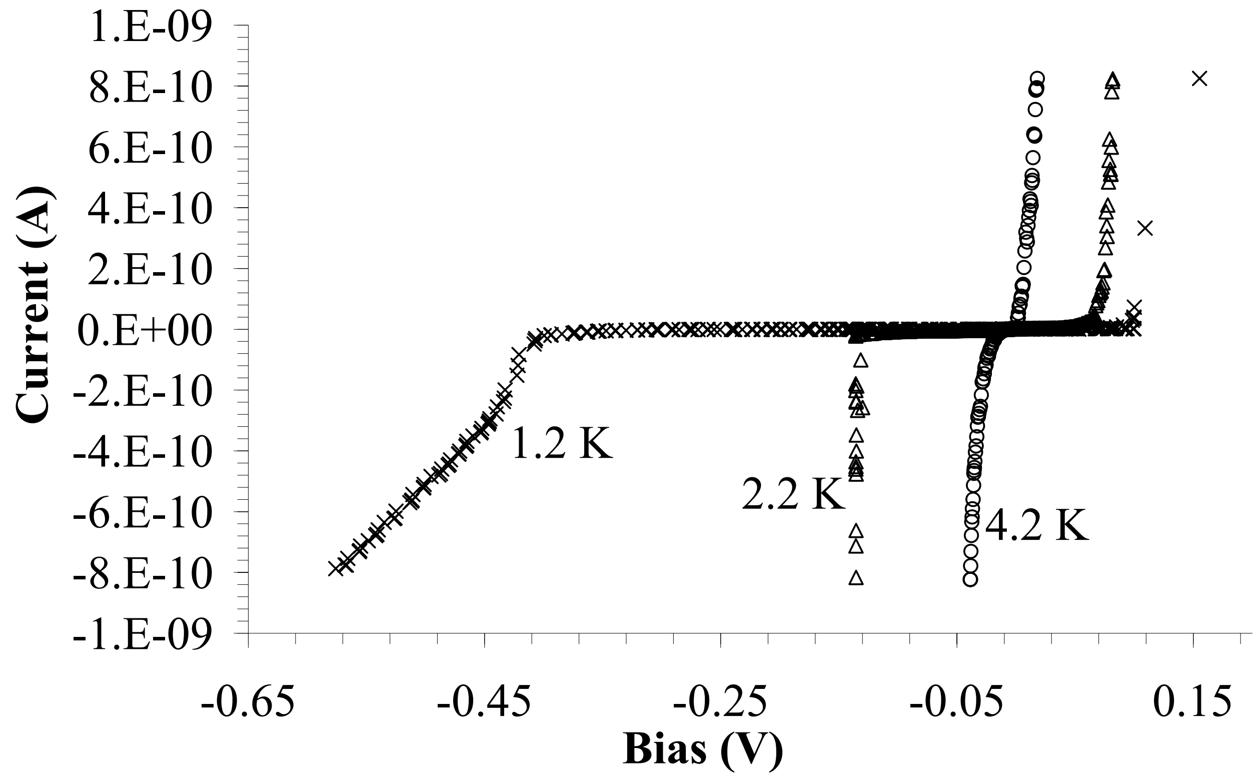

Figure 6
J. Beeman et al.

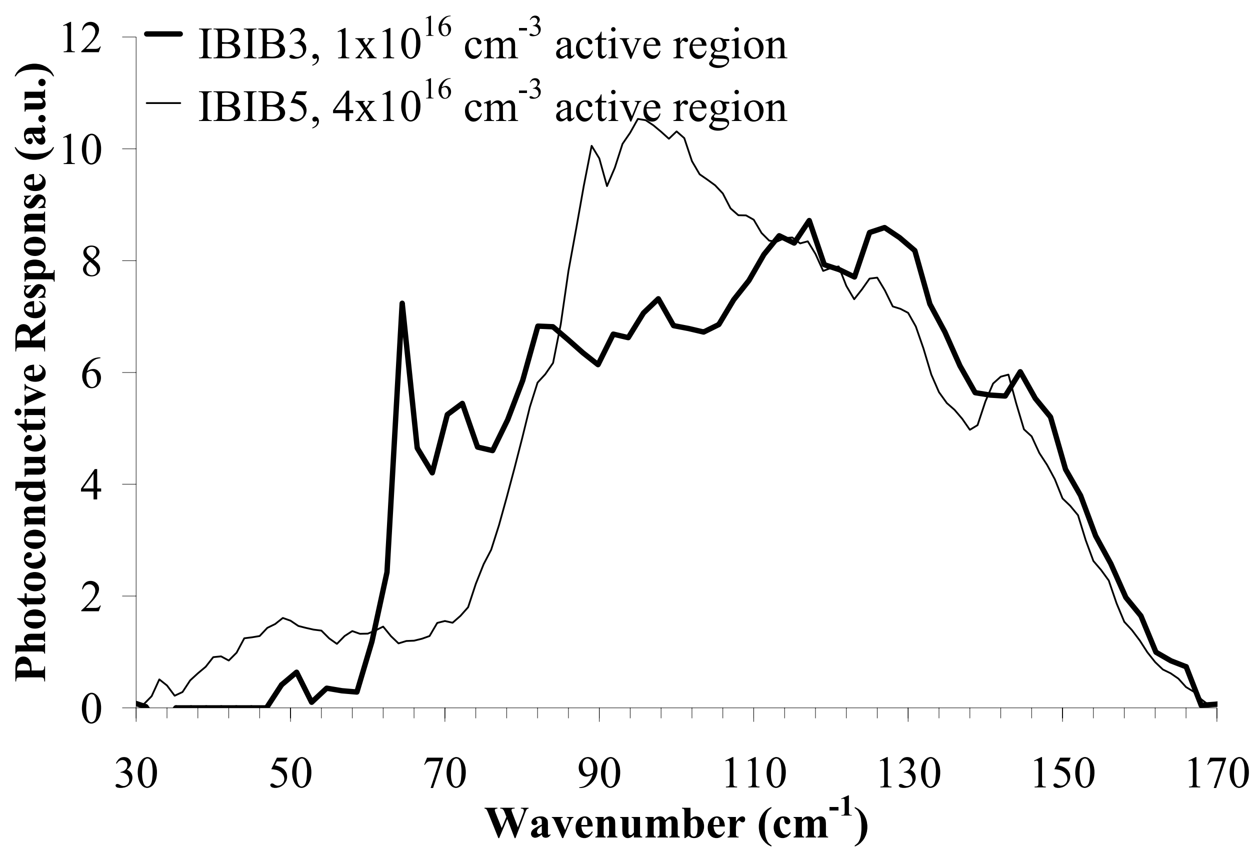

Figure 7
J. Beeman et al.

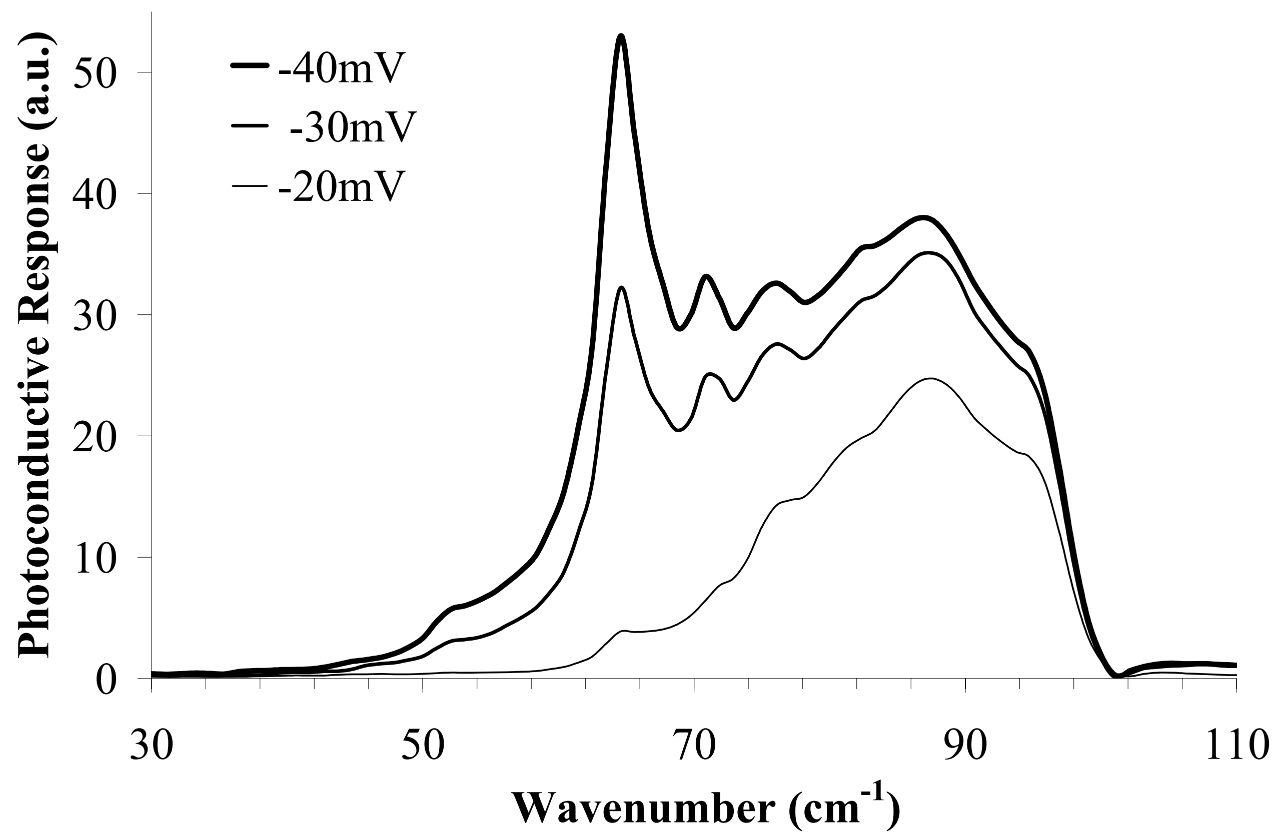

Figure 8
J. Beeman et al.